CO_2 Activation

DOI: 10.1002/ange.201409444

Spectroscopic Identification of a Bidentate Binding Motif in the Anionic Magnesium–CO_2 Complex ($[ClMgCO_2]^-$)**

Glenn B. S. Miller, Tim K. Esser, Harald Knorke, Sandy Gewinner, Wieland Schöllkopf, Nadja Heine, Knut R. Asmis, and Einar Uggerud**

Abstract: *A magnesium complex incorporating a novel metal–CO_2 binding motif is spectroscopically identified. Here we show with the help of infrared photodissociation spectroscopy that the complex exists solely in the $[ClMg(\eta^2\text{-}O_2C)]^-$ form. This bidentate double oxygen metal–CO_2 coordination has previously not been observed in neutral nor in charged unimetallic complexes. The antisymmetric CO_2 stretching mode in $[ClMg(\eta^2\text{-}O_2C)]^-$ is found at 1128 cm^{-1}, which is considerably redshifted from the corresponding mode in bare CO_2 at 2349 cm^{-1}, suggesting that the CO_2 moiety has a considerable negative charge (~1.8 e^-). We also employed electronic structure calculations and kinetic analysis to support the interpretation of the experimental results.*

Although not a new concept, the activation of carbon dioxide by metal (M) complexes is currently receiving much interest with regard to improving the feasibility of using CO_2 as a carbon feedstock in chemical synthesis.[1] This is an attractive prospect with regard to CO_2's abundance, and as a contribution to solving the environmental challenges associated with it; several reviews have summarized the progress.[2] Due to its role in carbon–carbon bond forming reactions, magnesium is of special interest. For example, in nature it is at the center of the active site in the plant protein RuBisCO which catalyzes C–C bond formation during the addition of a CO_2 molecule to a carbohydrate substrate.[3] Additionally, it plays a fundamental role in the classic Grignard reaction which is well known in organic chemistry.[4]

[*] G. B. S. Miller, Prof. Dr. E. Uggerud
Massespektrometrilaboratoriet and Senter for teoretisk og beregningsbasert kjemi (CTCC)
Kjemisk institutt, Universitetet i Oslo
Postboks 1033 Blindern, 0315 Oslo (Norway)
E-mail: einar.uggerud@kjemi.uio.no

T. K. Esser, H. Knorke, Prof. Dr. K. R. Asmis
Wilhelm-Ostwald-Institut für Physikalische und Theoretische Chemie
Universität Leipzig
Linnéstr. 2, 04103 Leipzig (Germany)
E-mail: knut.asmis@uni-leipzig.de

T. K. Esser, H. Knorke, S. Gewinner, Dr. W. Schöllkopf, Dr. N. Heine
Fritz-Haber-Institut der Max-Planck-Gesellschaft
Faradayweg 4-6, 14195 Berlin (Germany)

[**] We are grateful to the Norwegian Research Council (grant no. 179568/V30), the German Research Foundation DFG (SFB 1109), and the Norwegian Supercomputing Program (NOTUR) for a grant of computer time (grant no. NN4654K).

Supporting information for this article is available on the WWW under http://dx.doi.org/10.1002/anie.201409444.

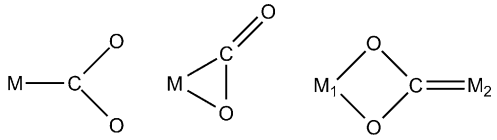

Scheme 1. The metal–CO_2 coordination modes $M(\eta^1\text{-}CO_2)$ (A) and $M(\eta^2\text{-}CO_2)$ (B) are the most common. Coordination as in (C) has only been observed in bimetallic complexes.

A key piece of information in understanding the reactivity of metal–CO_2 complexes is the coordination of CO_2 to the metal. In neutral complexes containing a single metal atom monodentate coordination $M(\eta^1\text{-}CO_2)$ or bidentate coordination $M(\eta^2\text{-}CO_2)$ are most common, corresponding to structures (A) and (B) in Scheme 1, respectively.[5] Linear "end-on" coordination is also seen, but is less common.[5b] Work on isolated anionic metal–CO_2 complexes is scarce, but $[M^-(CO_2)_n]^-$ complexes also prefer the coordination modes A and B, retaining a bent CO_2 moiety as a result of the partial negative charge transfer into the π^* orbital of CO_2.[6] In contrast, cationic metal–CO_2 complexes, $[M^-(CO_2)_n]^+$, have so far shown to exclusively coordinate CO_2 "end-on" to the metal due to the electron deficiency resulting in electrostatic bonding between the positively charged metal atom and the partial negative charge on oxygen in CO_2.[7] Here, we present first spectroscopic evidence of an anionic unimetallic Mg-containing complex with a bidentate double oxygen $M(\eta^2\text{-}O_2C)$ coordination, a binding motif that has, so far, only been encountered in bimetallic complexes (structure (C) in Scheme 1).

Mass spectrometric evidence was recently presented suggesting the presence of the bidentate motif (C) in anionic Mg-containing complexes of the type $[XMgCO_2]^-$, in which X = Cl, Br, OH. These complexes are formed by electrospraying a solution of oxalic acid and a Mg^{2+} salt (MgX_2, X = Cl, Br).[8] The mass spectra show that the X = OH complex is reactive in S_N2 gas phase reactions, providing support for the bidentate $[HOMg(\eta^2\text{-}O_2C)]^-$ structure analogous to structure **1** in Figure 1. However, the G4-level calculations included in that paper[8c] suggest the presence of an additional isomer $[HOMg(\eta^2\text{-}CO_2)]^-$ with the more classic structure (B), analogous to structure **2** in Figure 1, which is 32 kJ mol^{-1} higher in energy than **1**. Based on this information it is not clear which of the isomers is observed in the experiment, as not only the energetics of the minimum energy structures but also the barrier heights along the reaction coordinate need to

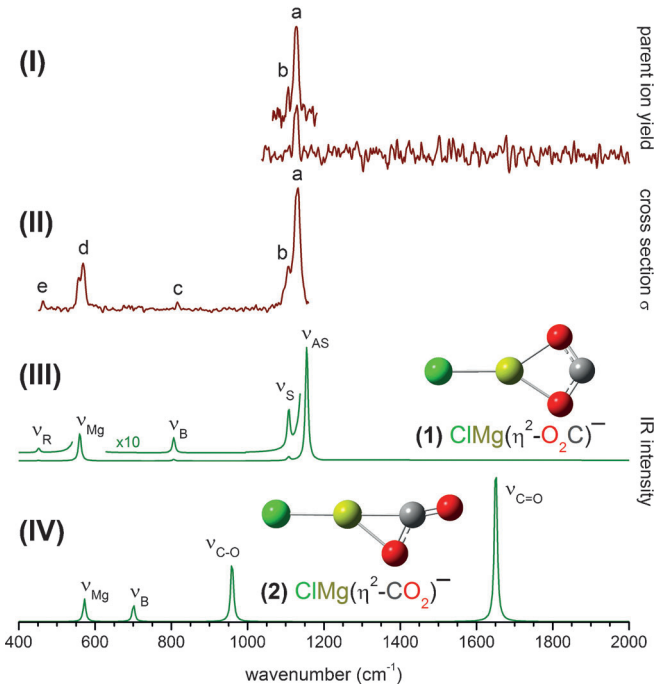

Figure 1. Comparison of vibrational predissociation spectra of $ClMgCO_2^-\cdot D_2$, measured with the table-top laser system from 1050 to 2000 cm^{-1} (I) and with the FHI-FEL from 450 to 1140 cm^{-1} (II) to simulated IR spectra for the (**1**) $[ClMg(\eta^2\text{-}O_2C)]^-$ (III), and (**2**) $[ClMg(\eta^2\text{-}CO_2)]^-$ isomers (IV). The additional trace shown above trace I was measured with a smaller step size and longer accumulation times, yielding an improved signal/noise ratio. See text and Table 1 for band assignments.

be considered. We have now conducted infrared photodissociation (IRPD) spectroscopy on the X = Cl complex, $[ClMgCO_2]^-$, to pin down the preferred binding motif of these complexes based on their vibrational fingerprint.

Vibrational spectra of $[ClMgCO_2]^-$, measured by way of IR vibrational predissociation spectroscopy of the $[ClMgCO_2]^-\cdot D_2$ complex (see the Experimental Section for details), are presented in the top part of Figure 1. Two IRPD spectra are shown probing overlapping regions, in which the higher energy region is covered with a table-top laser system (I, 1050–2000 cm^{-1}) and the lower energy region with the FHI-FEL IR free electron laser[9] (II, 450–1130 cm^{-1}). From the inspection of trace I it is directly apparent that the characteristic absorptions of the coordination modes A and B, typical for anionic metal–CO_2 complexes,[6,10] between 1650 and 1900 cm^{-1} are absent from this spectrum. The highest energy IRPD band is observed at 1128 cm^{-1}, labeled (a) in Figure 1, followed by peaks (b)–(e) (see Table 1 for band assignments) at lower energies.

To aid in the assignment of the vibrational spectra we performed electronic structure calculations and simulated linear absorption spectra derived from unscaled harmonic vibrational frequencies and intensities for structures **1** and **2**. All the employed theoretical methods (see Experimental Section for details) predict essentially the same vibrational normal modes and representatively the MP2/aug-cc-pVTZ spectra (traces III and IV) are shown in Figure 1. The

Table 1: Experimental IRPD band positions (in cm^{-1}), computed unscaled harmonic frequencies, and band assignments for $[ClMg(\eta^2\text{-}O_2C)]^-$.

Experiment	CCSD(T)[a]	MP2[b]	wB97XD[b]	Assignment
1128 (a)	1139	1155	1216	CO_2 antisym. stretch (ν_{AS})
1106 (b)	1105	1108	1171	CO_2 sym. stretch (ν_S)
814 (c)	816	806	849	CO_2 bend (ν_B)
570 (d)	560	560	568	ClMgC stretch (ν_{Mg})
463 (e)	459	452	475	CO_2 rock (ν_R)
MSE[c]	5	10	41	n/a

[a] aug-cc-pVTZ, untagged; [b] aug-cc-pVTZ, tag on oxygen; [c] mean signed error; n/a not applicable.

experimental IRPD band positions, calculated IR frequencies, and band assignments are summarized in Table 1.

The simulated spectrum of **1** (trace III) satisfactorily recovers the position and relative intensity of all five observed bands, whereas no evidence is found for **2** (trace IV). The two strongest IRPD bands at 1128 cm^{-1} (a) and 570 cm^{-1} (d) correspond to the antisymmetric CO_2 stretching (ν_{AS}) and Cl-Mg-C stretching (ν_{Mg}) modes, respectively. Peaks characteristic for **1** are also detected at 1106 cm^{-1} (b), 814 cm^{-1} (c), and 462 cm^{-1} (e) and assigned to the CO_2 symmetric stretch (ν_S), bend (ν_B), and rock (ν_R), respectively. For comparison, the most intense IR transitions of **2** are predicted at 1700 cm^{-1} (free C=O stretch), and at 950 cm^{-1} (bound C–O stretch), at which no corresponding features are present in the experimental spectra.

The position of the antisymmetric CO_2 stretching mode ν_{AS} yields additional information on the amount of charge transfer in the complex. In bare CO_2, ν_{AS} is found at 2349 cm^{-1}. Addition of an electron to CO_2 leads to a weakening of the C=O bonds, a distortion from the linear geometry, and a redshift of ν_{AS}, which is proportional to the extent of charge transfer. While CO_2^- by itself is not stable in the gas phase with respect to electron autodetachment ($EA = -0.6$ eV), its IR spectrum has been measured in a Ne matrix, yielding a value for ν_{AS} of 1658.3 cm^{-1}.[11] Intermediate values for ν_{AS} (1865–1680 cm^{-1}) have been found in CO_2-solvated $M(CO_2)^-$ complexes (M = Au, Ag), thus corresponding to partial charge transfers ranging from 0.5 to 0.9 e^-.[6b,10] The observation of a considerably more redshifted ν_{AS} for **1** (1128 cm^{-1}) suggests that substantially more negative charge (~1.8 e^-) is transferred to the CO_2 moiety in $[ClMgCO_2]^-$. This analysis then yields a CO_2^{2-} ligand with strong carbene character.

We also performed calculations on neutral $[Mg\text{–}CO_2]$ to see if the chloride is directing the CO_2 coordination in $[ClMgCO_2]^-$. Both MP2/aug-cc-pVTZ and G4 find only $[Mg(\eta^2\text{-}O_2C)]$ as a stable complex, with no minimum found for $[Mg(\eta^2\text{-}CO_2)]$, suggesting that the chloride does not alter the CO_2-coordinating properties of magnesium.

Energetically, **1** is favored by 29 kJ mol^{-1} over **2**; however, the formation mechanism and reaction barriers also need to be considered. The potential energy surface, calculated at the G4 level, along with the kinetic analysis presented in Figure 2 provide further support for the exclusive presence of isomer **1**. Both isomers **1** and **2** follow similar mechanisms beginning

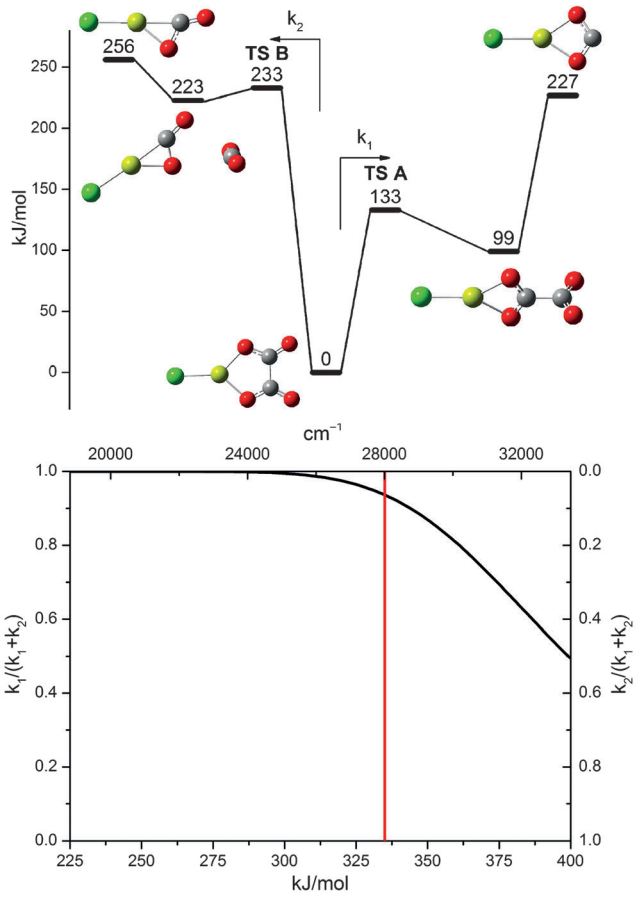

Figure 2. G4 potential energy surface (top) describing the formation of $[ClMg(\eta^2\text{-}O_2C)]^-$ and $[ClMg(\eta^2\text{-}CO_2)]^-$. The bottom graph shows the ratio of the rate coefficients $k(E)$ (calculated with RRKM theory) for the formation of each isomer. The vertical red line marks the dissociation energy (335 kJ mol^{-1}) of both $[ClMgCO_2]^-$ complexes.

with the isomerization of the $[ClMgC_2O_4]^-$ precursor. Once isomerization is complete via either **TS A** or **TS B**, CO_2 is lost producing isomer **1** or **2**, respectively. Formation of $[ClMg(\eta^2\text{-}O_2C)]^-$ via **TS A** is greatly favored due to its much lower isomerization barrier of 133 kJ mol^{-1}, which is 100 kJ mol^{-1} lower than the corresponding barrier of **TS B** leading to $[ClMg(\eta^2\text{-}CO_2)]^-$. The effect of this difference is clearly reflected in the kinetic analysis, because the formation of $[ClMg(\eta^2\text{-}CO_2)]^-$ is not competitive until energies (> 335 kJ mol^{-1}) are reached that significantly exceed the dissociation threshold of both complexes.

In summary, we have shown that the $[ClMg(\eta^2\text{-}O_2C)]^-$ complex exhibits a bidentate coordination of CO_2, in which both oxygen atoms are bound to Mg, a result which is consistent with the high oxophilicity and hardness of the Mg^{2+} ion.[12] This may elucidate some of the intrinsic interactions of the biologically important Mg^{2+} ion with an activated CO_2 molecule, because the CO_2 moiety in our complex has a considerable negative charge giving its carbon a highly nucleophilic character as a result of this binding scheme.

Experimental Section

The IRPD experiments were performed using the Berlin 6 K ion-trap triple mass spectrometer[13] in combination with the widely tunable and intense IR radiation from the free electron laser FHI-FEL.[9] Gas-phase anions were produced using a nanospray ion-source from a solution of oxalic acid (1 mM) and magnesium chloride (2 mM) in a 1:1 water/methanol mixture. $[ClMgCO_2]^-$ anions were obtained from $[ClMgC_2O_4]^-$ through skimmer collision-induced dissociation. Parent ions were mass-selected and focused into a cryogenically cooled radio frequency ring-electrode ion-trap. To allow for continuous ion loading and thermalization, the trap was continuously filled with D_2 gas at a trap temperature of 14.5 K. The untagged $[ClMgCO_2]^-$ and messenger-tagged $[ClMgCO_2]^-\cdot(D_2)$ ions were then extracted from the ion trap and irradiated with the IR laser pulse prior mass spectrometric detection. The FHI-FEL was operated from 450–1200 cm^{-1} with a bandwidth of approximately 4 cm^{-1} and an average power of 6 mJ per macropulse. The IRPD spectra were recorded by monitoring all ion intensities simultaneously as the laser wavelength was scanned. The photodissociation cross-section σ was determined as described previously.[14] Additional measurements in the range from 1000 to 2000 cm^{-1} were performed using the radiation from an IR OPO/OPA table-top laser system.[15] The laser pulses had a bandwidth of ~3 cm^{-1} and an average pulse energy of 0.7 mJ. The resulting IRPD spectra reflect the total parent ion signal (instead of σ), to avoid additional noise due to the normalization procedure at low laser pulse energies.

A range of density functional theory (DFT) functionals and the wavefunction methods MP2 and CCSD(T) were employed to simulate the experimental IRPD spectra. The DFT and MP2 calculations were performed with the Gaussian 09 program package, whereas the CCSD(T) calculations were performed with the MOLPRO and CFOUR program packages.[16] Briefly, the most accurate harmonic frequencies were obtained at the CCSD(T)/aug-cc-pVTZ level of theory, and the best relative intensities were obtained at the DFT levels of theory. The kinetic analysis was performed using the Rice–Ramsperger–Kassel–Markus (RRKM) theory using MP2/aug-cc-pVTZ rovibrational data and G4 energies.[16d,17]

Received: September 24, 2014
Revised: October 8, 2014
Published online: October 27, 2014

Keywords: carbon dioxide · IR spectroscopy · magnesium · mass spectrometry · structure elucidation

[1] a) M. Aresta, A. Dibenedetto, *Dalton Trans.* **2007**, 2975–2992; b) M. Cokoja, C. Bruckmeier, B. Rieger, W. A. Herrmann, F. E. Kühn, *Angew. Chem. Int. Ed.* **2011**, *50*, 8510–8537; *Angew. Chem.* **2011**, *123*, 8662–8690.
[2] a) D. H. Gibson, *Chem. Rev.* **1996**, *96*, 2063–2096; b) D. H. Gibson, *Coord. Chem. Rev.* **1999**, *185–186*, 335–355; c) X. Yin, J. R. Moss, *Coord. Chem. Rev.* **1999**, *181*, 27–59; d) M. Mikkelsen, J. Mikkel, F. C. Krebs, *Energy Environ. Sci.* **2010**, *3*, 43–81.
[3] a) R. J. Ellis, *Trends Biochem. Sci.* **1979**, *4*, 241–244; b) I. Andersson, *J. Exp. Bot.* **2008**, *59*, 1555–1568.
[4] V. Grignard, *Ann. Chim. Phys.* **1901**, *24*, 433.
[5] a) F. A. Cotton, G. Wilkinson, C. A. Murillo, M. Bochmann, *Advanced Inorganic Chemistry*, *6 ed.*, Wiley, New York, **1999**; b) see Ref. [1b].
[6] a) A. D. Boese, H. Schneider, A. N. Glöß, J. M. Weber, *J. Chem. Phys.* **2005**, *122*, 154301; b) B. J. Knurr, J. M. Weber, *J. Phys. Chem. A* **2013**, *117*, 10764–10771; c) B. J. Knurr, J. M. Weber, *J. Phys. Chem. A* **2014**, *118*, 4056–4062.

[7] a) C. S. Yeh, K. F. Willey, D. L. Robbins, J. S. Pilgrim, M. A. Duncan, *J. Chem. Phys.* **1993**, *98*, 1867 – 1875; b) R. S. Walters, N. R. Brinkmann, H. F. Schaefer, M. A. Duncan, *J. Phys. Chem. A* **2003**, *107*, 7396 – 7405; c) J. B. Jaeger, T. D. Jaeger, N. R. Brinkmann, H. F. Schaefer, M. A. Duncan, *Can. J. Chem.* **2004**, *82*, 934 – 946; d) N. R. Walker, R. S. Walters, M. A. Duncan, *J. Chem. Phys.* **2004**, *120*, 10037 – 10045; e) G. Gregoire, M. A. Duncan, *J. Chem. Phys.* **2002**, *117*, 2120 – 2130; f) N. R. Walker, R. S. Walters, G. A. Grieves, M. A. Duncan, *J. Chem. Phys.* **2004**, *121*, 10498 – 10507; g) R. L. Asher, D. Bellert, T. Buthelezi, P. J. Brucat, *Chem. Phys. Lett.* **1994**, *227*, 623 – 627.

[8] a) S. Curtis, J. Renaud, J. Holmes, P. Mayer, *J. Am. Soc. Mass Spectrom.* **2010**, *21*, 255 – 256; b) A. B. Attygalle, F. U. Axe, C. S. Weisbecker, *Rapid Commun. Mass Spectrom.* **2011**, *25*, 681 – 688; c) H. Dossmann (Soldi-Lose), C. Afonso, D. Lesage, J.-C. Tabet, E. Uggerud, *Angew. Chem. Int. Ed.* **2012**, *51*, 6938 – 6941; *Angew. Chem.* **2012**, *124*, 7044 – 7047.

[9] W. Schöllkopf, W. Erlebach, S. Gewinner, G. Heyne, H. Junkes, A. Liedke, G. Meijer, V. Platschkowski, G. v. Helden, *Proc. FEL 2013* **2013**.

[10] B. J. Knurr, J. M. Weber, *J. Am. Chem. Soc.* **2012**, *134*, 18804 – 18808.

[11] a) R. N. Compton, P. W. Reinhardt, C. D. J. Cooper, *J. Chem. Phys.* **1975**, *63*, 3821; b) W. E. Thompson, M. E. Jacox, *J. Chem. Phys.* **1999**, *111*, 4487.

[12] R. G. Pearson, *J. Am. Chem. Soc.* **1963**, *85*, 3533 – 3539.

[13] N. Heine, Ph.D. Thesis, Freie Universität Berlin (Germany), **2014**.

[14] N. Heine. T. I. Yacovitch, T. Schubert, C. Brieger, D. M. Neumark, K. R. Asmis, *J. Phys. Chem. A* **2014**, *118*, 7613 – 7622.

[15] W. R. Bosenberg, D. R. Guyer, *J. Opt. Soc. Am. B* **1993**, *10*, 1716 – 1722.

[16] a) (Gaussian 09, Revision D.01), M. J. Frisch, et al., Gaussian, Inc., Wallingford, CT, USA, **2009**; b) H.-J. Werner, P. J. Knowles, G. Knizia, F. R. Manby, M. Schütz, *Wiley Interdiscip. Rev. Comput. Mol. Sci.* **2012**, *2*, 242 – 253; c) M. E. Harding, T. Metzroth, J. Gauss, A. A. Auer, *J. Chem. Theory Comput.* **2008**, *4*, 64; d) Please see the Supporting Information for details.

[17] R. G. Gilbert, S. C. Smith, *Theory of Unimolecular and Recombination Reactions*, Blackwell Scientific Publications, Oxford, **1990**.

